Soft Matter

Accepted Manuscript

ROYAL SOCIETY OF CHEMISTRY

www.rsc.org/softmatter

Graphical abstract

The trimer forms an achiral ground-state conformer in the nematic phase, but by intermolecular interactions between cores it adopts a twisted chiral conformer to exhibit the spontaneous mirror symmetry breaking in the low-temperature DC phase.

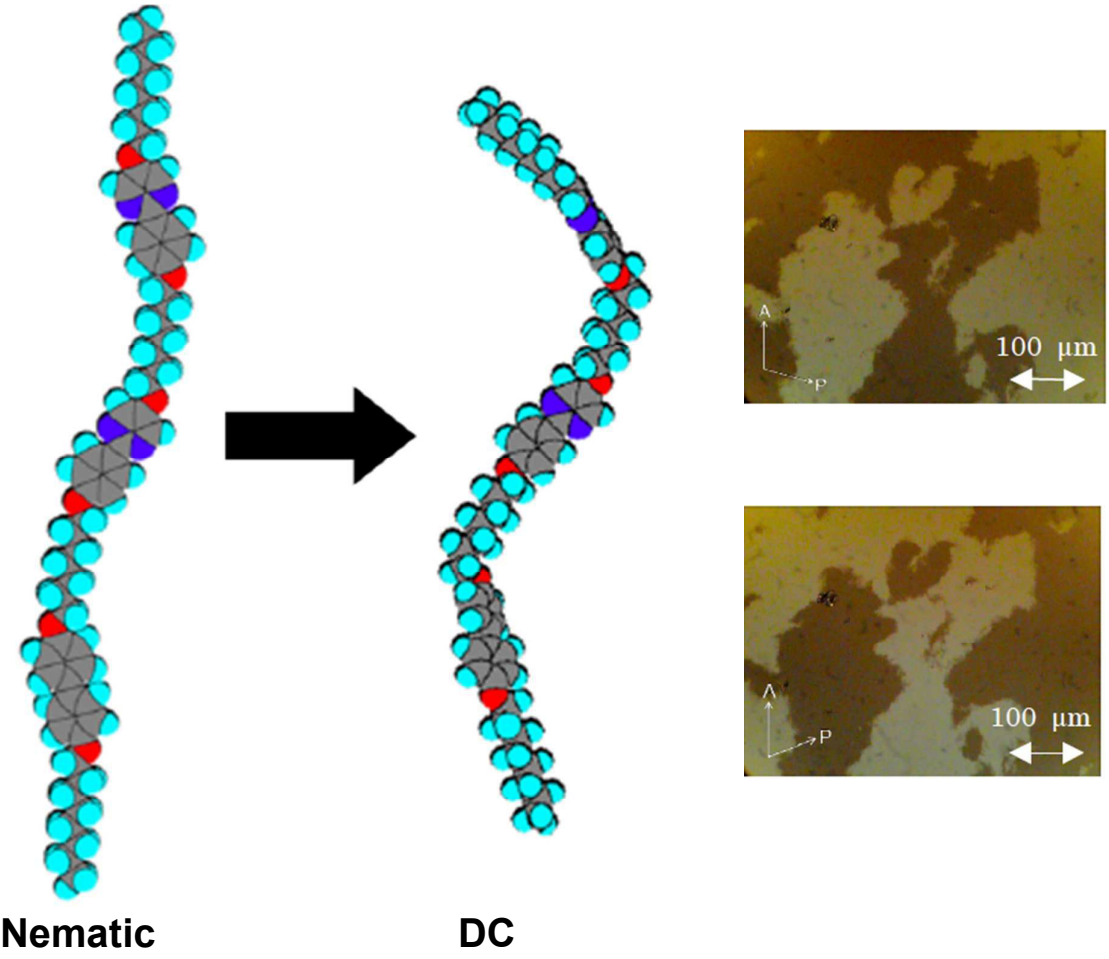

Achiral flexible liquid crystal trimers exhibiting chiral conglomerates

Haruna Sasaki,[a] Yoichi Takanishi,[b] Jun Yamamoto[b] and Atsushi Yoshizawa*,[a]

[a]Department of Frontier Materials Chemistry, Graduate School of Science and Technology, Hirosaki University, 3 Bunkyo-cho, Hirosaki, 036-8561, Japan
E-mail: ayoshiza@hirosaki-u.ac.jp
[b]Department of Physics, Graduate School of Science, Kyoto University, Oiwake-cho, Kitashirakawa, Sakyo-ku, Kyoto, 606-8502, Japan

Abstract

Chiral conglomerates of domains with opposite handedness have attracted much attention from researchers. We prepared a homologous series of achiral liquid crystal trimers in which two phenylpyrimidine units and one biphenyl unit are connected via flexible methylene spacers. We investigated their phase transition behaviour. Some trimers possessing odd-numbered spacers were found to exhibit a nematic phase and a dark chiral conglomerate phase possessing a layer structure. The chiral characteristics were confirmed by uncrossing the polarizers in opposite directions. Layer spacing detected using X-ray diffraction was about 80% of the molecular length. Structure–property relations indicate that intermolecular interactions cause conformation change of the trimer possessing flexible odd-numbered methylene spacers to form a helical conformer with axial chirality, which might induce chiral segregation and layer deformation to drive the chiral conglomerates.

Introduction

Spontaneous mirror symmetry breaking in soft matter has attracted much attention from researchers.[1] Chiral conglomerates consisting of domains with opposite handedness have been observed recently not only in liquid crystalline phases[2–14] but also in isotropic liquids.[15] The spontaneous mirror symmetry breaking results from 1) chiral discrimination of permanently chiral molecules, 2) chiral synchronization of transiently chiral molecules capable adopting chiral conformations representing energy minima, or 3) chiral synchronization of prochiral molecules which have an achiral ground-state conformation, but which easily adopt chiral conformations.[1,16] Chiral synchronization in lamellar liquid-crystalline phases engenders dark conglomerate phases (DC phases) that have been observed in some achiral bent-shaped molecules. Depending on the local structure of these DC phases, they are classifiable as liquid-crystalline sponge phases,[5, 17–19] formed by strongly deformed fluid layers, or as helical nanofilament phases (HNF phases, also assigned as B4 phases).[2,7,8,20–22] The sponge phases, usually formed during cooling of the isotropic liquid, have little or no birefringence. The texture under crossed polarizers is nearly dark. Such phases are macroscopically isotropic sponge-like soft solids. The application of high voltage transforms some of such phases to B2 phase.[5,19] The HNF phase is apparently a solid phase, with in-plane hexatic positional ordering of the layers[6] and short-range layer order.[6] Although no electro-optical switching can be found in the HNF phase, it is SHG active,[4] indicating the existence of polar order in the phase. Results of earlier studies have demonstrated that the smectic layers in both the sponge phases and HNF phases of bent-core liquid crystals tend to have saddle splay curvature.[5,6] The optical activity in the DC phases has been investigated extensively, revealing that it is attributable to the layer chirality[23] or to the coupling of molecular conformational chirality to the layer chirality.[20] Furthermore, DC phases of new types including modifications of the HNF phase have been observed.[24–27] Almost all molecules exhibiting the DC phases have a rigid bent-core structure, except in a few cases in which the HNF phase of an achiral dimer possessing an odd-numbered spacer was reported.[28–31] The ground-state conformer of the rigid molecule influences the origin of the chirality. Such bent-core molecules tend to form layer structures, and they not often exhibit a nematic phase. Chiral conglomerate formation is thought to be due to chirality synchronization of the transiently chiral bent-shaped molecules.[1,3,7,8] Fundamental interest persists in the unusual phenomena related to the DC phases. Materials exhibiting the DC phase can support important applications such as organic semiconductors and organic photovoltaics.[32] Actually, material design for the DC phase

is an attractive subject.

Recently, we found an equimolecular mixture of achiral liquid crystal trimers exhibiting the HNF phase, suggesting that dipole–dipole interactions between adjacent cores plays an important role in the appearance of HNF phase.[33] Furthermore, HNF was induced in binary mixtures of an achiral nematic liquid crystal trimer possessing a central biphenyl unit and **6OCB**. Interaction between a phenylpyrimidine unit of trimer **1** and a cyanobiphenyl unit of **6OCB** can produce a twist conformation of the central biphenyl of the trimer, which induces chiral segregation and layer deformation to drive the chiral conglomerate.[34] This report describes some achiral liquid crystal trimers possessing odd-numbered spacers exhibiting a DC phase. We discuss how the molecular structures affect the spontaneous mirror symmetry breaking.

Experimental

Materials

Spectroscopic Analysis. The purity of each final compound was confirmed using elemental analysis (EA 1110; CE Instruments Ltd.). Infrared (IR) spectroscopy (FTS-30; Bio-Rad Laboratories Inc.) and proton nuclear magnetic resonance (^{1}H NMR) spectroscopy (JNM-ECA500; JEOL) elucidated the structure of the final product.

Preparation of Materials. For use in this study, 5-hydroxy-2-(4-hydroxyphenyl)pyrimidine and 5-hydroxy-2-(4-octyloxyphenyl)pyrimidine were purchased from Midori Kagaku Co. Ltd. An achiral liquid crystal trimer, 2-{4-[7-(4-(4-octyloxyphen-1-yl)phenyloxy)heptyloxy]phenyl}-5-{7-[4-(5-octyloxypyri-midin-2-yl)phenyloxy]heptyloxy}pyrimidine (**I–(7,7)**), was prepared by the synthesis outlined in Fig. 1.

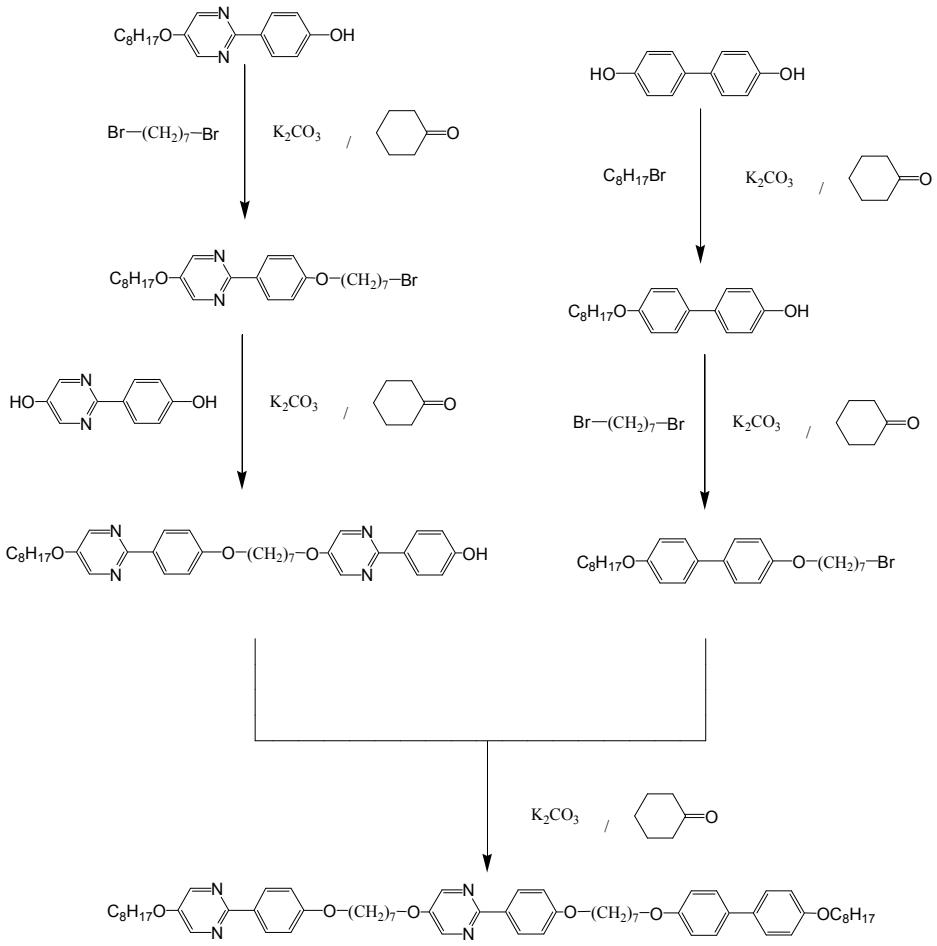

Fig. 1 Synthesis of compound **I–(7,7)**.

2-{4-[7-(4-(4-Octyloxyphenyl)phenyloxy)heptyloxy]phenyl}-5-{7-[4-(5-octyloxypyrimidin-2-yl)phenyloxy]heptyloxy}pyrimidine (I–(7,7)).

Potassium carbonate (1.5 mmol, 207 mg) was added to a solution of 2-(4-hydroxyphenyl)-5-octyloxypyrimidine (1.5 mmol, 451 mg) and 1,7-dibromoheptane (2.25 mmol, 600 mg) in cyclohexanone (20 ml). The reaction mixture was stirred at 95 °C for 8 h. After filtration of the precipitate, the solvent was removed by evaporation. Then the residue was purified using column chromatography on silica gel with a hexane : ethyl acetate (4:1) mixture as the eluent. The obtained white solid was recrystallized from hexane to give 5-octyloxy-2-{4-(7-bromoheptyloxy)phenyl}pyrimidine. Yield 358 mg (50%).

Potassium carbonate (1.25 mmol, 138 mg) was added to a solution of 2-(4-hydroxyphenyl)-5-pyrimidinol (1.25 mmol, 235 mg) and

5-octyloxy-2-{4-(7-bromoheptyloxy)phenyl}pyrimidine (1.0 mmol, 477.5 mg) in cyclohexanone (20 ml). The reaction mixture was stirred at 95 ℃ for 6 h. After filtration of the precipitate, the solvent was removed by evaporation. Then the residue was purified using column chromatography on silica gel with a dichloromethane : ethyl acetate (8:1) mixture as the eluent. The obtained white solid was recrystallized from ethanol to give 2-(4-hydroxyphenyl)-5-{7-[4-(5-octyloxypyrimidin-2-yl)phenyloxy]heptyloxy}pyrimidine. Yield 367 mg (63%).

Potassium carbonate (2.0 mmol, 276 mg) was added to a solution of 4,4'-biphenol (2.5 mmol, 466 mg) and 1-bromooctane (2.0 mmol, 386 mg) in cyclohexanone (10 ml). The reaction mixture was stirred at 95 ℃ for 6 h. After filtration of the precipitate, the solvent was removed by evaporation. Then the residue was purified using column chromatography on silica gel with a toluene: ethyl acetate (3:1) mixture as the eluent. The obtained white solid was washed with hexane to give 4-(4-octyloxyphenyl)phenol. Yield 243 mg (41%).

Potassium carbonate (0.74 mmol, 102 mg) was added to a solution of 4-(4-octyloxyphenyl)phenol (0.74 mmol, 220 mg) and 1,7-dibromohexane (0.93 mmol, 239 mg) in cyclohexanone (10 ml). The reaction mixture was stirred at 95 °C for 10 h. After filtration of the precipitate, the solvent was removed by evaporation. Then the residue was purified using column chromatography on silica gel with a hexane : ethyl acetate (5:1) mixture as the eluent. The obtained white solid was recrystallized from ethanol to give 1-(4-octyloxyphenyl)-4-(7-bromoheptyloxy)benzene. Yield 181 mg (51%).

Potassium carbonate (0.15 mmol, 21 mg) was added to a solution of 1-(4-octyloxyphenyl)-4-(7-bromoheptyloxy)benzene (0.15 mmol, 71 mg) and 2-(4-hydroxyphenyl)-5-{7-[4-(5-octyloxypyrimidin-2-yl)phenyloxy]heptyloxy}pyrimidine (0.15 mmol, 90 mg) in cyclohexanone (10 ml). The reaction mixture was stirred at 130 °C for 10 h. After filtration of the precipitate, the solvent was removed by evaporation. Then the residue was washed with hot ethanol and was recrystallized from toluene to give the desired compound. Yield 112 mg (76%).

^{1}HNMR (500 MHz, $CDCl_3$, TMS): δ=8.40 (s, 4H, Ar-**H**), 8.26 (d, 4H, Ar-**H**, *J* = 9.2 Hz), 7.44 (d, 4H, Ar-**H**, *J* = 6.9 Hz), 6.96 (d, 4H, Ar-**H**, *J* = 8.6 Hz), 6.93 (d, 4H, Ar-**H**, *J* = 8.6 Hz), 4.08 (t, 2H, -OC**H$_2$**-), 4.07 (t, 2H, -OC**H$_2$**-), 4.03 (t, 2H, -OC**H$_2$**-), 4.02 (t, 2H, -OC**H$_2$**-), 3.99 (t, 2H, -OC**H$_2$**-), 3.98 (t, 2H, -OC**H$_2$**-), 1.86–1.76 (m, 12H, aliphatic-**H**), 1.53–1.29 (m, 32H, aliphatic-**H**), 0.89 (t, 6H, -C**H$_3$**, *J* = 6.9 Hz). IR (KBr):ν cm^{-1}: 2938, 2854 (C-H str), 1607 (Ar-H str), 1251 (C-O str). Elemental analysis calcd. for C,76.0; H,

8.44; N, 5.72. Found C, 75.3; H, 8.53; N, 5.66.

Characterization of the other trimers is listed in Supporting Information.

Liquid-crystalline and physical properties

The initial phase assignments and corresponding transition temperatures for each final compound were determined using a polarizing optical microscope (POM, BX-51; Olympus Optical Co. Ltd.) equipped with a temperature control unit (LK-600PM; Japan High Tech Co. Ltd.). The temperatures and enthalpies of transition were investigated using differential scanning calorimetry (DSC, DSC 6200; Seiko Instruments Inc.). The X-ray diffraction patterns of the homeotropically aligned sample during cooling were obtained using a real-time X-ray diffractometer (MicroMax–007HF; Rigaku Corp.) equipped with a hot stage and a temperature-control processor. A sample was put on a convex lens, which was then placed in a custom-made temperature-stabilized holder (stability within ±0.1 °C). The phase transition of the sample under the X-ray beam was monitored by observing the texture simultaneously using polarized light microscopy with a CCD camera. The X-ray apparatus was equipped with a platform arrangement and a two-dimensional detector (Image intensifier and CCD C9299–01; Hamamatsu Photonics KK) for small-angle X-ray scattering (SAXS), and an imaging plate (BAS-SR 127; Fujifilm) for wide-angle X-ray scattering (WAXS). Then X-rays were generated at 40 kV and 20 mA. The sample was irradiated with a Cu-Kα X-ray beam, using confocal mirrors to correlate the incident X-ray beam and to increase its intensity. Camera distances from the samples to the detectors were ca. 730 mm for SAXS and 40 mm for WAXS.

The correlation length along the layer normal (ξ) was determined using the Ornstein−Zernike expression as follows. First, the X-ray profile as a function of 2θ was converted to a scattering function of q according to the following equation.

$$q = (4\pi/\lambda) \sin\theta \qquad (1)$$

By fitting the X-ray profiles using the following Lorentzian equation, the correlation length ξ was determined.

$$I(q) = \frac{I_0}{1+(q-q_0)^2\xi^2} + \text{background} \qquad (2)$$

Therein, I_0 and q_0 respectively signify the peak height and the peak position of q.

Electro-optical properties were measured using standard electro-optical techniques. The ITO-coated glass sandwich cells purchased from EHC Corp. were constructed with 2 μm spacers. The ITO electrodes were covered with a polymer

alignment layer, rubbed unidirectionally.

Results and discussion

Physical properties of I–(7,7)

We designed trimer **I–(7,7)**, in which two phenylpyrimidine units and a biphenyl unit were connected via heptamethylene spacers. We investigated its phase transition behaviour using polarized optical microscopy (POM) and differential scanning calorimetry (DSC).

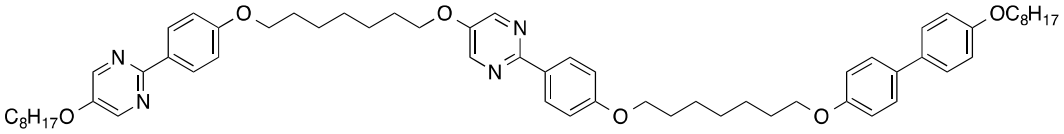

I–(7,7)

Phase transition temperatures and $\Delta S/R$ of trimer **I–(7,7)** were the following: Iso 155.8 °C (1.2) N 146.4 °C (10.4) DC. The DC phase did not change until 0 °C. When on heating of a virgin sample , the crystal (Cry_1)–crystal (Cry_2) transition was observed at 144.0 °C (5.5). Then the Cry_2 changed to the N phase at 135.2 °C and then it changed to the Iso at 156.9 °C (8.8). In the Cry_1 and Cry_2 phases, no chiral nature was detected. The DSC thermogram is portrayed in Fig. 2.

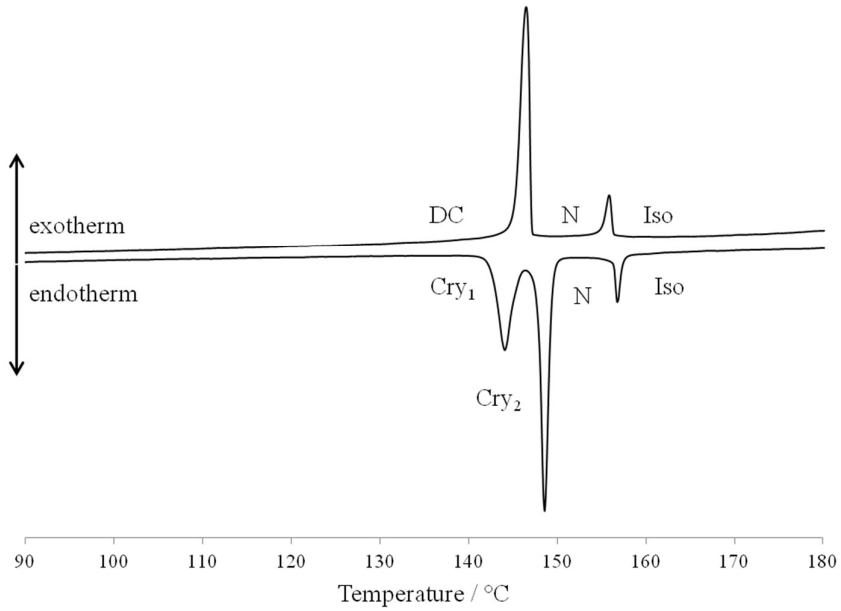

Fig. 2 DSC thermogram of trimer **I–(7,7)**. The rate of cooling and heating was 5 °C min^{-1}.

Fig. 3 shows the optical textures of trimer **I–(7,7)** in the DC phase at 130 °C under crossed and uncrossed polarizers. The texture of the DC phase under crossed polarizers was nearly dark, suggesting that it is optically isotropic. By observing the sample in the DC phase under slightly uncrossed polarizers (10°), the texture was split into darker and brighter domains. By uncrossing the polarizers in opposite directions by the same angle, the darker and brighter domains were exchanged. The domain brightness did not change by rotation of the sample between the polarizers. These results indicate that they have optical activity with opposite senses. With respect to the N phase above the DC phase, no chiral nature was detected. Chiral aggregation occurs at the N to DC phase transition.

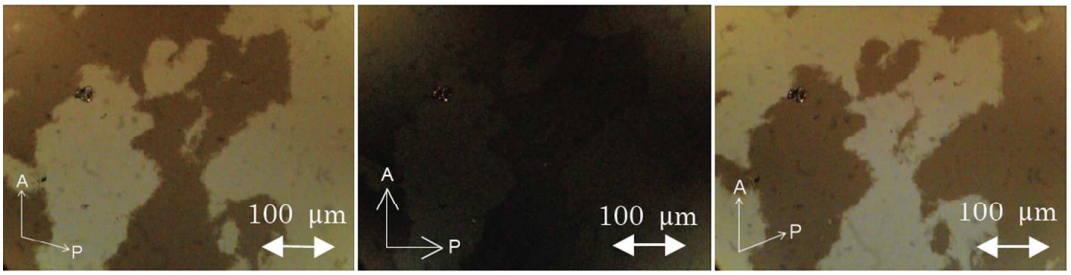

Fig. 3 Polarized optical textures of trimer **I–(7,7)** on a glass slide with a cover glass in

the DC phase at 130 °C with uncrossed and crossed polarizers.

We investigated the electro-optical response in the DC phase by application of an AC field to the sample in a homogeneously aligned cell with a gap of 2 μm using a triangle wave with an AC field of ±30 V μm^{-1} at a frequency of 10 Hz. Electro-optical switching was not observed in the DC phase.

To elucidate the phase structure, X-ray measurements were conducted. Alignment was performed by the slow cooling of a small drop of the sample on a convex lens. The N to DC phase transition was confirmed by the texture change. Fig. 4(a) portrays an X-ray diffraction pattern in the small-angle region of trimer **I–(7,7)** in the DC phase at $T - T_{NDC} = -13.0$ K (T_{NDC}: N−DC transition temperature). In the DC phase, weak and broad scattering appeared in a circle. Fig. 4(b) depicts an X-ray diffraction profiles in the small-angle region of trimer **I–(7,7)** in the N and DC phases. A diffuse scattering at around $2\theta = 1.41°$ can be seen in the N phase at $T - T_{NDC} = 10.0$ K, suggesting that a short-range order with a periodicity length of about 62 Å exists in the N phase. Therefore the N phase is not a cybotactic N phase,[35,36] which is often seen in a bent-core liquid crystal, but a conventional N phase. A peak at $2\theta = 1.56°$ was observed in the DC phase, revealing that the DC phase has a layer structure with a periodicity length of 56.5 Å. Correlation length for the periodicity in the small-angle region in DC phase is 350 Å at $T - T_{NDC} = -13.0$ K, which corresponds to about six layers. Fig. 5 (a) shows an X-ray diffraction pattern in the wide-angle region of trimer **I–(7,7)** in the DC phase. Fig. 5(b) shows profiles in the wide-angle region of trimer **I–(7,7)** in the N and DC phases. Four peaks $2\theta = 14.8°$, 19.4°, 23.5°, and 27.5° were observed in the DC phase, as portrayed in Fig. 5(b), indicating that it has positional order within the layer. No other peak was detected in the middle-angle and wide-angle regions. These results reveal that the DC phase is a crystalline structure.

(a) (b)

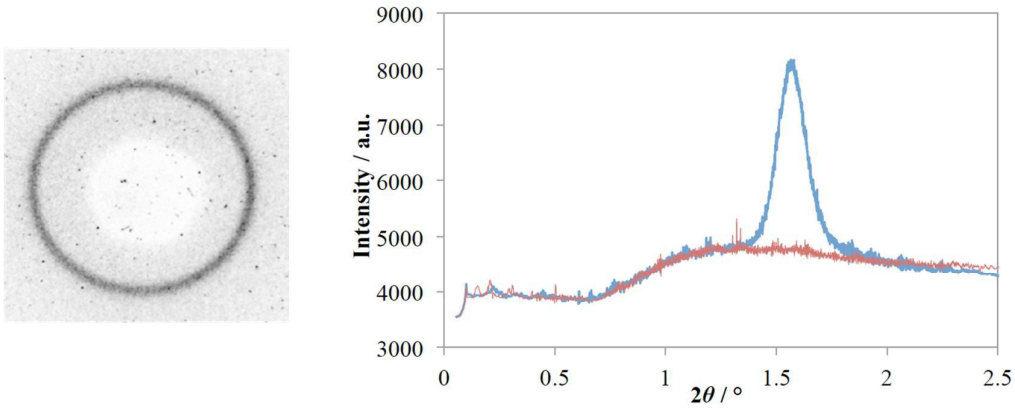

Fig. 4 (a) X-ray diffraction pattern of trimer **I–(7,7)** in the DC phase at $T–T_{NDC} = –13.0$ K in the small-angle region. (b) X-ray diffraction profiles of trimer **I–(7,7)** in the N phase at $T–T_{NDC} = 10.0$ K (red line) and the DC phase at $T–T_{NDC} = –13.0$ K (blue line) in the small-angle region.

(a) (b)

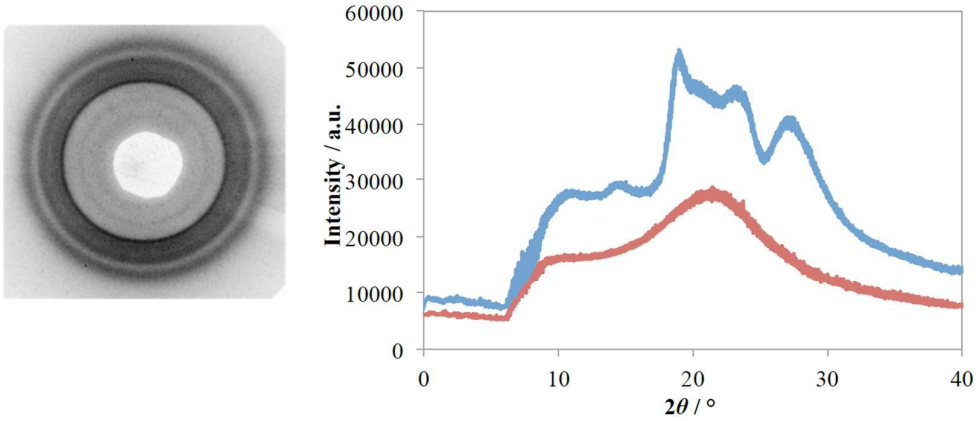

Fig. 5 (a) X-ray diffraction pattern of trimer **I–(7,7)** in the DC phase at $T–T_{NDC} = –13.0$ K in the wide-angle region. (b) X-ray diffraction profiles of trimer **I–(7,7)** in the N phase at $T–T_{NDC} = 10.0$ K (red line) and the DC phase at $T–T_{NDC} = –13.0$ K (blue line) in the wide-angle region.

Fig. 6 portrays the temperature dependence of the periodicity length in the DC phase. The layer spacing at T_{NDC} is 56.7 Å. The layer spacing decreases with decreasing temperature in the DC phase. It reaches a value of 56.2 Å at $T - T_{NDC} = −28.0$ K. The layer spacing corresponds to the length of the trimer and not to the length of the single

mesogenic unit, indicating the segregation of spacers and terminal chains.

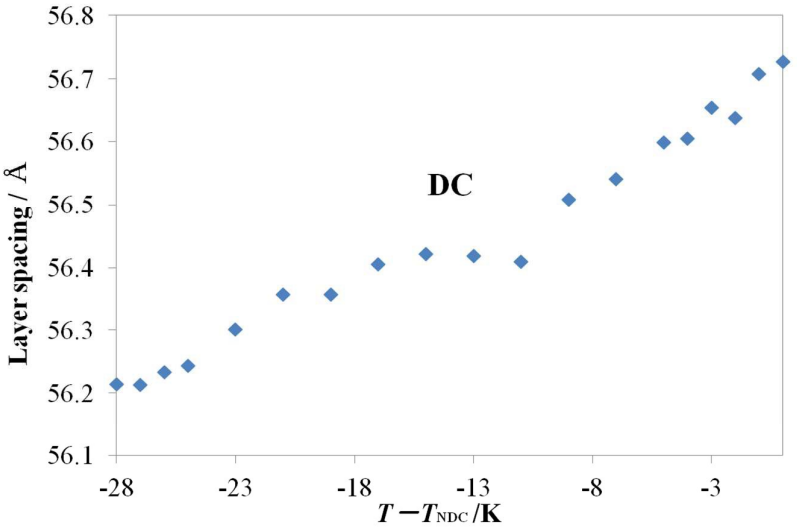

Fig. 6 Temperature dependence of the periodicity length in the DC phase of trimer **I–(7,7)**.

Fig. 7 (a) shows that an extended molecular length for trimer **I–(7,7)** with all trans conformation of the spacers is estimated by semi-empirical calculations using MOPAC-6/PM3 to be 68 Å. The layer spacing is shorter than the molecular length. The difference between layer spacing and molecular length is possible by molecular tilt with respect to the layer normal, conformational chain disorder, and chain interdigitation. The tilt angle based on the XRD measurements is estimated as 26° if the trimer is tilted with the layer normal. The layer periodicity of 62.3 Å in the SmA phase of trimer **III–(7,7)** described later was used as a basis for the calculation of the tilt angle. On the other hand, this large difference between the layer spacing and molecular length is found similarly for the DC phases of the related 4-iodo and 4-methylresorcinol derivatives.[26,27] Layer spacing in the previously reported HNF phases is usually close to the molecular length. The shorter layer spacing observed for some resorcinol bent-core LCs is explained in terms of the twisted conformation of the bent-core molecule.[27] Structure–property relations of the resorcinol bent-core mesogens reveal that conformation chirality attributable to the rigid twist structure plays an important role in the appearance of the DC phase.[27] The molecular length is estimated as 57 Å if compound **I–(7,7)** has a twisted conformation, as portrayed in Fig. 7 (b). The origin for the difference between layer spacing and molecular length will be discussed later.

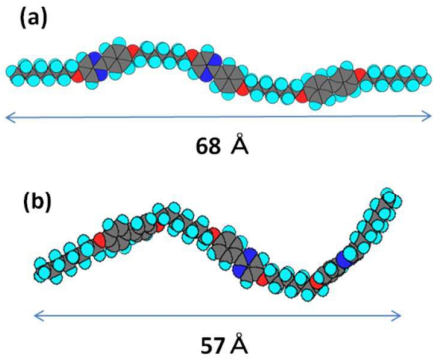

Fig. 7 MOPAC models for trimer **I–(7,7)** with (a) extended conformation and (b) twisted conformation.

Trimer **I–(7,7)** exhibited sharp peaks in the wide-angle region and showed no electrooptical switching in the DC phase, suggesting that the DC phase is an HNF phase. It can be swollen in a nematic liquid crystal if the DC phase is an HNF phase.[37–39] However, a binary mixture of **I–(7,7)** (50 wt%) and **6OCB** (50 wt%) exhibited the following phase transition: Iso 132 °C Iso + N 118 °C Cry. Phase separation occurred instead of dilution of the DC phase. A molecular length for **6OCB** is estimated using MOPAC to be 18 Å. Trimer **I–(7,7)** is 3.8 times the length of **6OCB**, hence efficient packing might just not be possible, thus a nematic phase is formed. The HNF phases can be swollen up to >90% with a nematic liquid crystal and retain a DC structure. Therefore, the DC phase of trimer **I–(7,7)** is not an HNF phase but more similar to a soft crystalline DC phase.[26,27]

Effects of spacer length

We prepared a homologue series of trimer **I–(n,m)** with different spacer lengths and investigated their phase transition behaviour. The results are presented in Fig. 8. Phase transition temperatures and entropies are listed in Supporting Information (Table S1). Trimers **I–(7,9)** and **I–(9,9)** exhibited a phase sequence of Iso–N–DC, as did trimer **I–(7,7)**. However, trimer **I–(5,5)** showed no mesogenic phase. Trimer **I–(7,5)** exhibited N and SmC phases. Then it crystallized without the DC phase. Trimer **I–(6,6)**, possessing even-numbered spacers, exhibited SmC and unidentified smectic phases. If we assume that spacers of those trimers form all trans conformation, a trimer with odd-numbered spacers has a zigzag shape in which all three mesogenic units are inclined with respect to each other, whereas a trimer with even-numbered spacers has a linear shape in which

the three mesogenic units are coparallel. Generally, the flexibility of a liquid crystal trimer increases with increasing spacer length. Therefore, coupling between zigzag sharp and flexibility is thought to play an important role in the appearance of the DC phase.

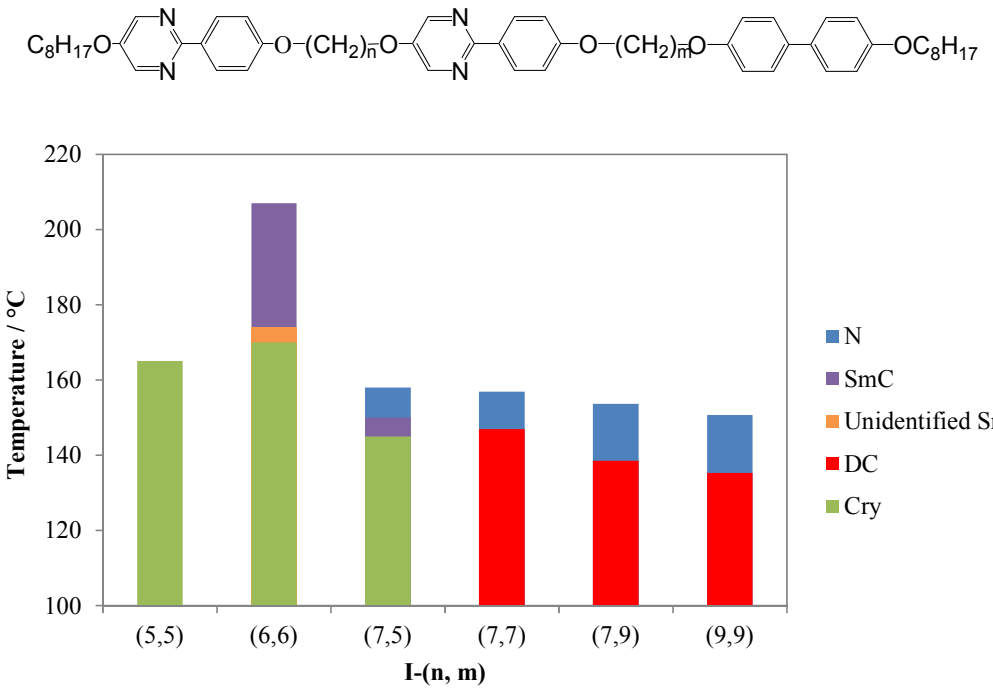

Fig. 8 Phase diagram for homologue series of trimer **I–(n,m)**.

Effects of core structures

To elucidate the mechanism by which intermolecular interactions between odd-membered trimers contribute to the appearance of the DC phase, we prepared some derivatives of trimer **I–(7,7)** and investigated their phase transition behaviour. The molecular structures and the phase transition properties are presented in Fig. 9. Trimer **II–(7,7)** exhibited N and DC phases just as they did for trimer **I–(7,7)**. No significant difference is apparent in their mutual transition properties. Both trimers **III–(7,7)** and **IV–(7,7)** exhibited a phase sequence of Iso–SmA–SmC–SmX–Y. SmX and Y phases are unidentified phases. They showed neither N phase nor DC phase. They do not form nematic phases. Polarized optical textures and DSC thermogram of trimer **III–(7,7)** are shown in Fig. S1 and Fig. S2, respectively. Schlieren texture in the homeotropic aligned region changed to mosaic texture at the SmC–SmX transition, however, no enthalpy

change was detected. The SmX phase is though to be one of smectic C sub-phases. On the other hand, the SmX–Y transition accompanied both a marked texture change and a large transition enthalpy. Further investigation is necessary to identify the Y phase.

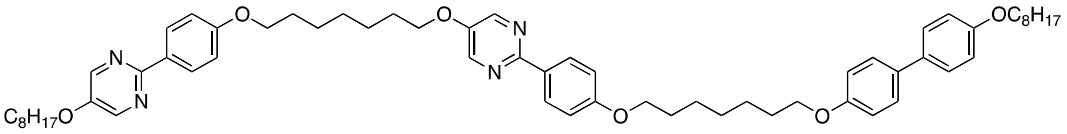

I–(7,7)

Heating: Cry_1 144.0 (5.5) Cry_2 135.2 (8.8) N 156.9 (1.2) Iso
Cooling: Iso 155.8 (1.2) N 146.4 (10.4) DC

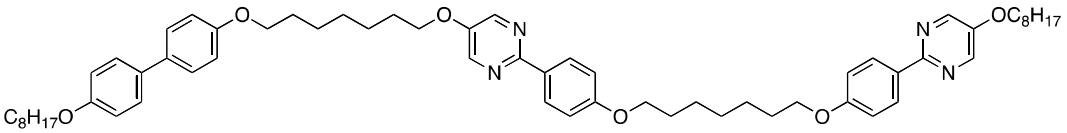

II–(7,7)

Heating: Cry_1 137.0 (6.2) Cry_2 142.6 (8.3) N 155.6 (1.4) Iso
Cooling: Iso 154.5 (1.4) N 140.8 (8.6) DC 112.7 (2.6) Cry

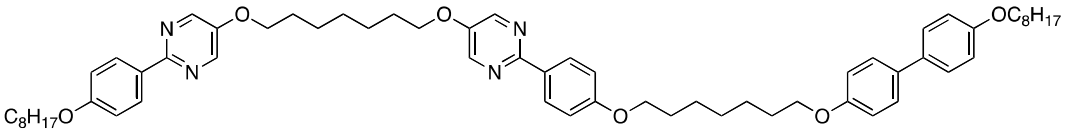

III–(7,7)

Heating: Cry 120.4 (4.5) Y 137.5 (4.1) SmX 144.8 (–)[a] SmC 157.6 (–)[a] SmA 162.6 (4.2) Iso
Cooling: Iso 160.6 (4.2) SmA 153.7 (–)[a] SmC 143.5 (–)[a] SmX 139.4 (5.4) Y 99.0 (3.3) Cry

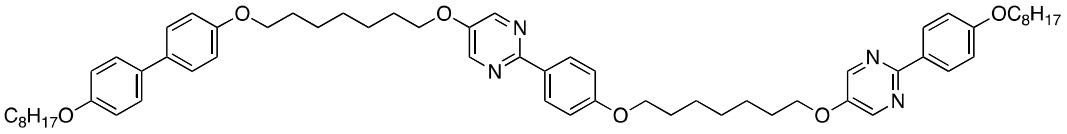

IV–(7,7)

Heating: Cry 133.8 (4.2) Y 142.9 (5.7) SmX 145.8 (–)[a] SmC 160.8 (–)[a] SmA 164.0 (5.6) Iso
Cooling: Iso 163.1 (6.0) SmA 159.4 (–)[a] SmC 144.4 (–)[a] SmX 140.5 (6.5) Y 121.3 (8.7) Cry

Fig. 9 Molecular structures, phase transition temperatures (°C), and $\Delta S/R$ in parentheses. Square brackets denote a monotropic transition. SmX and Y phases are unidentified phases. [a]Entropy changes too small to be detected.

Fig. 10 shows temperature dependence of the layer periodicity of trimer **III–(7,7)**. The layer spacing in the SmA phase of **III–(7,7)** at $T–T_{IsoA}$ = –5.0 K is 62.3 Å. It is shorter than the molecular length of 68 Å, suggesting interlayer permeation of terminal tails between adjacent layers. The layer spacing in the SmC phase at $T–T_{IsoA}$ = –17.0 K is 61.8 Å. The maximum layer contraction of 0.8% suggests that the biaxiality in the SmC phase is not attributed to tilt of the long axis but to the zigzag shape of three mesogenic units within a trimer. If the DC phase of trimer **I–(7,7)** has a tilted layer structure, the biaxiality is also attributed to the tilt of each mesogenic unit within the trimer as same as the SmC phase of trimer **III–(7,7)**. The layer spacings of trimer **I–(7,7)** in the DC phase are much shorter than those of **III–(7,7)** in the SmC phase. The difference between layer spacing and molecular length of trimer **I–(7,7)** cannot be explained only by the zigzag shape. Conformational disorder in the spacers might be the most important origin for the difference.

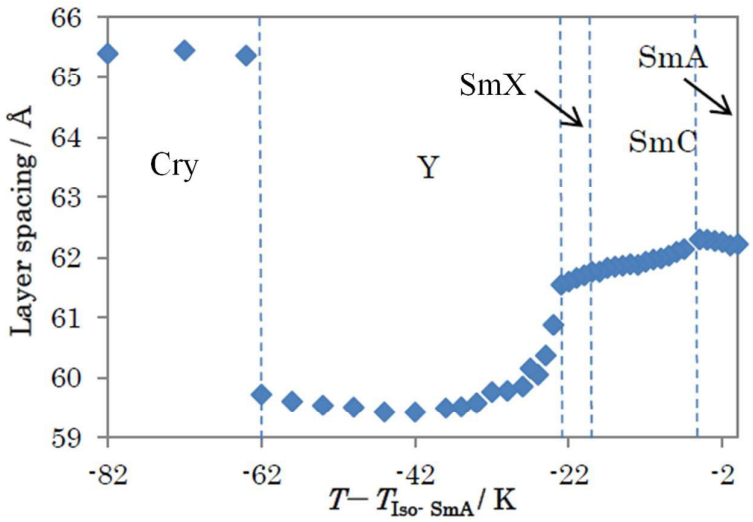

Fig. 10 Temperature dependence of the layer periodicity of trimer **III–(7,7)**.

Fig. 11 portrays models for the molecular organization of those trimers. We assume an antiparallel molecular packing organized by the core–core interaction between central phenylpyrimidine units in adjacent molecules. Core–core interactions of the antiparallel packing for **I–(7,7)** are the same as those for **II–(7,7)**. Those for **III–(7,7)** are the same as those for **IV–(7,7)**. These models can explain that trimers **I–(7,7)** and **II–(7,7)** have the same transition behaviour, and also that trimers **III–(7,7)** and **IV–(7,7)** have the

same transition behaviour. The molecular organization models are realistic. Next we discuss the differences in the transition behaviours of **I–(7,7)** and **III–(7,7)**. In comparison of the organization model between **I–(7,7)** and **III–(7,7)**, the difference is a position of pyrimidine in the outer phenylpyrimidine unit. We also consider that trimer **I–(7,9)** possessing different odd-numbered spacers shows the DC phase. We can say that dense molecular packing around the biphenyl unit is not favourable for the appearance of the DC phase.

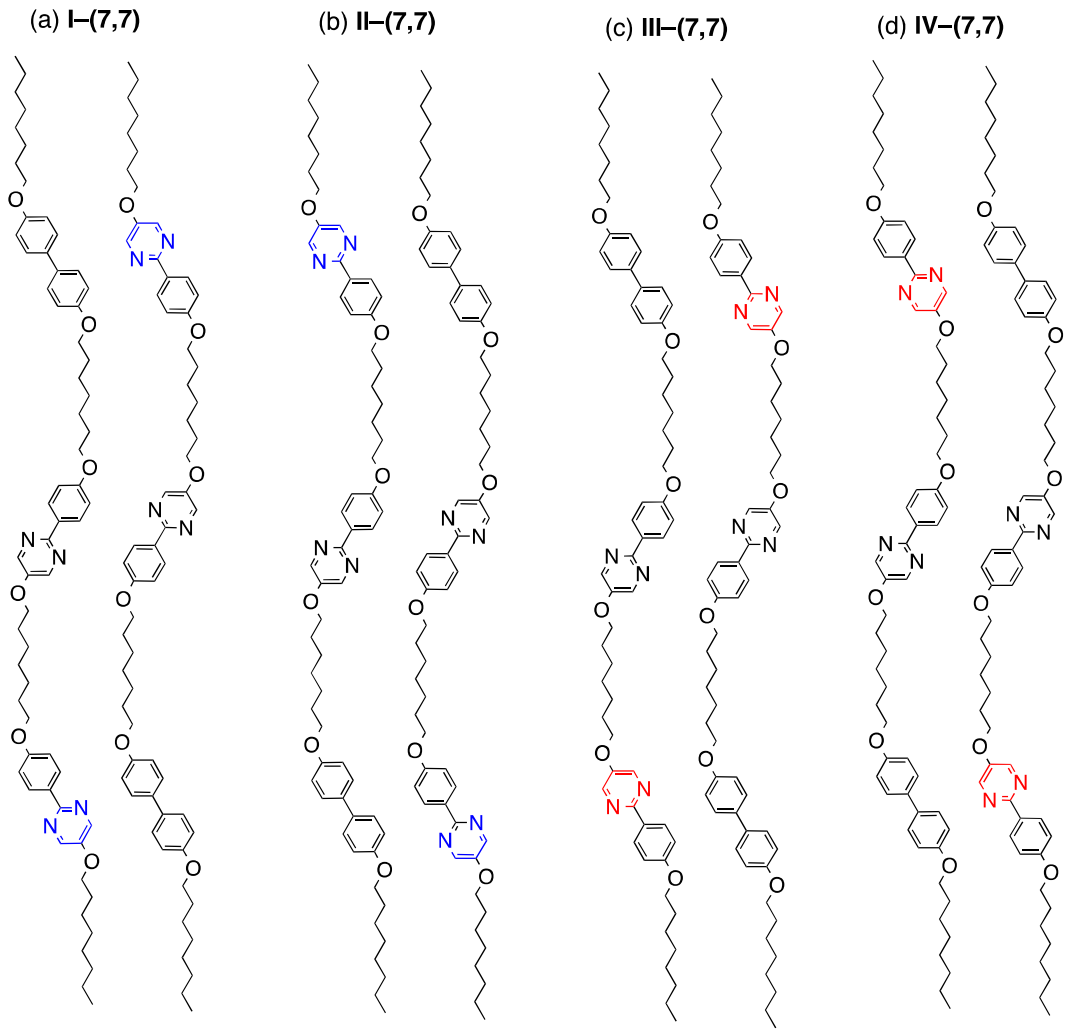

Fig. 11 Models for molecular organization of trimers **I–(7,7)**, **II–(7,7)**, **III–(7,7)** or **IV–(7,7)** in their layer structure.

Fig. 12 shows a possible model for the origin of chirality in the DC phase of trimer **I–(7,7)**. As described above, the trimers have a short-range periodicity of about 62 Å in

the N phase, whereas they have a layer peridodicity of 56.7 Å at T_{NDC}. Conformational disorder in the spacers of trimer **I–(7,7)** occurs at the N–DC phase transition. The dipole–dipole interaction between the antiparallel central phenylpyrimidine units might drive the layered structure. We surmise that the interaction between the biphenyl unit and the outer phenylpyrimidine unit for **I–(7,7)** is repulsive. The biphenyl unit of **I–(7,7)** can adopt the twisted conformation. The strong core–core interaction between the central phenylpyrimidine units is thought to restrict free rotation of the biphenyl axis of each trimer to produce axial chirality. The attractive interaction between the central cores and the repulsive interactions between outer cores can induce the conformational disorder in the spacers. Coupling between the axial chirality and the disordered odd-numbered spacers can produce a helical conformer. According to an explanation for the formation of soft crystalline DC phases,[26,27,40] the packing of helical conformers can produce macroscopic chirality, which induces twist and bend of the layers to lead to deformation or fragmentation of these layers.

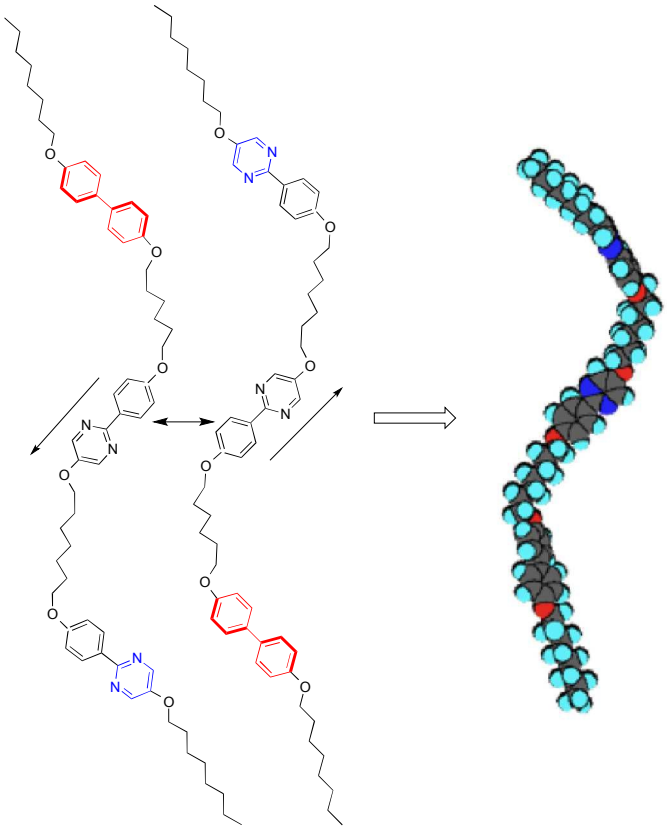

Fig. 12 Model for the origin of the chirality of **I–(7,7)** in the DC phase.

Conclusion

We prepared a homologous series of achiral liquid crystal trimers in which two phenylpyrimidine units and one biphenyl unit are connected via flexible methylene spacers. Some trimers possessing odd-numbered spacers were found to exhibit a crystalline DC phase of domains with opposite handedness. The trimer forms an achiral ground-state conformer in the nematic phase, but by intermolecular interactions between cores it adopts a chiral conformer to exhibit the spontaneous mirror symmetry breaking in the low-temperature DC phase.

References

1. C. Tschierske and G. Ungar, *ChemPhysChem*, 2016, **17**, 9.
2. H. Takezoe and Y. Takanishi, *Jpn. J. Appl. Phys.*, 2006, **45**, 597.
3. "Nanoscale Stereochemistry in Liquid Crystals": C. Tschierske in Chirality at the Nanoscale (Ed.: D. B. Amabilino), Wiley-VCH, Weinheim, 2009, pp. 271–304.
4. A. Eremin and A. Jakli, *Soft Matter*, 2013, **9**, 615.
5. L. E. Hough, M. Spannuth, M. Nakata, D. A. Coleman, C. D. Jones, G. Dantlgraber, C. Tschierske, J. Watanabe, E. Körblova, D. M. Walba, J. E. Maclennan, M. A. Glaser and N. A. Clark, *Science,* 2009, **325**, 452.
6. E. Hough, H. T. Jung, D. Kruerke, M. S. Heberling, M. Nakata, C. D. Jones, D. Chen, D. R. Link, J. Zasadzinski, G. Heppke, J. P. Rabe, W. Stocker, E. Korblova, D. M. Walba, M. A. Glaser and N. A. Clark, *Science*, 2009, **325**, 456.
7. H. Takezoe, *Top. Curr. Chem.*, 2012, **318**, 303.
8. R. A. Reddy and C. Tschierske, *J. Mater. Chem.*, 2006, **16**, 907.
9. V. P. Panov, M. Nagaraj, J. K. Vij, Y. P. Panarin, A. Kohlmeier, M. G. Tamba, R. A. Lewis, G. H. Mehl, *Phys. Rev. Lett.* 2010, **105**, 167801; V. Borshch, Y.-K. Kim, J. Xiang, M. Gao, A. Jakli, V. P. Panov, J. K. Vij, C. T. Imrie, M. G. Tamba, G. H. Mehl and O. D. Lavrentovich, *Nat. Commun.*, 2013, **4**, 2635.
10. M. Cestari, S. Diez-Berart, D. A. Dunmur, A. Ferrarini, M. R. de La Fuente, D. J. B. Jackson, D. O. Lopez, G. R. Luckhurst, M. A. Perez-Jubindo, R. M. Richardson, J. Salud, B. A. Timimi and H. Zimmermann, *Phys. Rev. E: Stat., Nonlinear, Soft Matter Phys.*, 2011, **84**, 031704.
11. D. Chen, J. H. Porada, J. B. Hooper, A. Klittnick, Y. Shen, M. R. Tuchband, E. Korblova, D. Bedrov, D. M. Walba, M. A. Glaser, J. E. Maclennan and N. A. Clark, *Proc. Natl. Acad. Sci. USA*, 2013, **110**, 15931.
12. V. Görtz and J. W. Goodby, *Chem. Commun*., 2005, 3262.
13. C. Roche, H.-J. Sun, M. E. Prendergast, P. Leowanawat, B. E. Partridge, P. A.

Heiney, F. Araoka, R. Graf, H. W. Spiess, X. B. Zeng, G. Ungar and V. Percec, *J. Am. Chem. Soc.*, 2014, **136**, 7169.
14. C. Dressel, F. Liu, M. Prehm, X.-B. Zeng, G. Ungar and C. Tschierske, *Angew. Chem. Int. Ed.*, 2014, **53**, 13115.
15. C. Dressel, T. Reppe, M. Prehm, M. Brautzsch and C. Tschierske, *Nat. Chem*., 2014, **6**, 971.
16. A. Zehnacker and M. Suhm, *Angew. Chem. Int. Ed.*, 2008, **47**, 6970.
17. J. Thisayukta, Y. Nakayama, S. Kawaguchi, H. Takezoe and J. Watanabe, *J. Am. Chem. Soc.*, 2000, **122**, 7441.
18. (a) H. Ocak, B. Bilgin-Eran, M. Prehm and C. Tschierske, *Soft Matter*, 2012, **8**, 7773; (b) H. Ocak, B. Bilgin-Eran, M. Prehm and C. Tschierske, *Soft Matter*, 2013, **9**, 4590.
19. M. Nagaraj, K. Usami, Z. Zhang, V. Görtz, J. W. Goodby and H. F. Gleeson, *Liq. Cryst.*, 2014, **41**, 800.
20. J. Thisayukta, H. Takezoe and J. Watanabe, *Jpn. J. Appl. Phys.*, 2001, **40**, 3277.
21. H. Niwano, M. A. Nakata, J. Thisayukta, D. R. Link, H. Takezoe and J. Watanabe, *J. Phys. Chem. B*, 2004, **108**, 14889.
22. D. Chen, J. E. Maclennan, R. Shao, D. K. Yoon, H. Wang, E. Körblova, D. M. Walba, M. A. Glaser, N. A. Clark, *J. Am. Chem. Soc.*, 2011, **133**, 12656.
23. D. R. Link, G. Natale, R. Shao, J. E. Maclennan, N. A. Clark, E. Körblova and D. M. Walba, *Science*, 1997, **278**, 1924.
24. E. Tsai, J. M. Richardson, E. Körblova, M. Nakata, D. Chen, Y. Shen, R. Shao, N. A. Clark and D. M. Walba, *Ang. Chem. Int. Ed.*, 2013, **52**, 5254.
25. G. B. Deepa, S. Radhika, B. K. Sadashiva and R. Pratibha, *Phys. Rev. E: Stat., Nonlinear, Soft Matter Phys.*, 2013, **87**, 062508.
26. M. Alaasar, M. Prehm, M. Brautzsch and C. Tschierske, *J. Mater. Chem. C*, 2014, **2**, 5487.
27. M. Alaasar, M. Prehm, M. Brautzsch and C. Tschierske, *Soft Matter*, 2014, **10**, 7285.
28. E. Bialecka-Florjanczk, I. Sledzinska, E. Gorecka and J. Przedmojski, *Liq. Cryst.*, 2008, **35**, 401.
29. T. Uda, S. Masuko, F. Araoka, K. Ishikawa and H. Takezoe, *Ang. Chem. Int. Ed.*, 2013, **52**, 6863.
30. A. Zep, M. Salamonczyk, N. Vaupotic, D. Pociecha and E. Gorecka, *Chem. Commun.,* 2013, **49**, 3119.
31. A. Zep, K. Sitkowska, D. Pociecha and E. Gorecka, *J. Mater. Chem. C*, 2014, **2**, 2323.

32. D. M. Walba, US 8,963,140 B2 (2013).
33. H. Sasaki, Y. Takanishi, J. Yamamoto and A. Yoshizawa, *J. Phys. Chem. B*, 2015, **119**, 4531.
34. A. Yoshizawa, Y. Kato, H. Sasaki, Y. Takanishi and J. Yamamoto, *Soft Matter*, 2015, **11**, 8827.
35. E. T. Samulski, *Liq. Cryst*., 2010, **37**, 669.
36. C. Tschierske and D. J. Photions, *J. Mater. Chem.*, 2010, **20**, 4283.
37. Y. Takanishi, G. J. Shin, J. C. Jung, S.-W. Choi, K. Ishikawa, J. Watanabe, H. Takezoe and P. Toledano, *J. Mater. Chem.*, 2005, **15**, 4020.
38. T. Otani, F. Araoka, K. Ishikawa and H. Takezoe, *J. Am. Chem. Soc.*, 2009, **131**, 12368.
39. Y. Takanishi, H. Yao, T. Fukasawa, K. Ema, Y. Ohtsuka, Y. Takahashi, J. Yamamoto, H. Takezoe and A. Iida, *J. Phys. Chem. B*, 2014, **118**, 3998.
40. M. Alaasar, M. Prehm and C. Tschierske, *Chem. Commun.*, 2013, **49**, 11062.